

Tidal Deformability of Strange Quark Planets and Strange Dwarfs

Xu Wang,¹ Abdusattar Kurban,² Jin-Jun Geng,³ Fan Xu,¹ Xiao-Li Zhang,⁴ Bing-Jun Zuo,⁴ Wen-Li Yuan,⁴ and Yong-Feng Huang^{1,5,*}

¹*School of Astronomy and Space Science, Nanjing University, Nanjing 210023, People's Republic of China*

²*Xinjiang Astronomical Observatory, Chinese Academy of Sciences, Urumqi 830011, Xinjiang, People's Republic of China*

³*Purple Mountain Observatory, Chinese Academy of Sciences, Nanjing 210023, People's Republic of China*

⁴*Department of Physics, Nanjing University, Nanjing 210093, People's Republic of China*

⁵*Key Laboratory of Modern Astronomy and Astrophysics (Nanjing University), Ministry of Education, Nanjing 210023, People's Republic of China*

(Accepted by PRD)

Strange quark matter, which is composed of u, d, and s quarks, could be the true ground state of matter. According to this hypothesis, compact stars may actually be strange quark stars, and there may even be stable strange quark dwarfs and strange quark planets. The detection of the binary neutron star merger event GW170817 provides us new clues on the equation of state of compact stars. In this study, the tidal deformability of strange quark planets and strange quark dwarfs are calculated. It is found to be smaller than that of normal matter counterparts. For a typical $0.6 M_{\odot}$ compact star, the tidal deformability of a strange dwarf is about 1.4 times less than that of a normal white dwarf. The difference is even more significant between strange quark planets and normal matter planets. Additionally, if the strange quark planet is a bare one (i.e., not covered by a normal matter crust), the tidal deformability will be extremely small, which means bare strange quark planets will hardly be distorted by tidal forces. Our study clearly proves the effectiveness of identifying strange quark objects via searching for strange quark planets through gravitational wave observations.

I. INTRODUCTION

The study of strong interaction at suprasaturation density is an important subject in modern physics. Ground-based experiments can place stringent constraints on the equation of state near the nuclear saturation density [1, 2]. However, the density at the center of neutron stars can be even higher than 5 times of the nuclear saturation density, of which the conditions cannot be imitated in laboratory [3, 4]. We thus have to resort to astronomical observations to probe the internal structure of compact stars. But due to the inaccuracy of the measurements of mass and radius for them, the equation of state (EoS) of compact stars is still highly uncertain [4].

In 2015, the Laser Interferometer Gravitational-wave Observatory (LIGO) detected the first gravitational wave event GW150914, which was produced by the merger of two black holes [5, 6]. The masses of the two black holes are $36_{-4}^{+5} M_{\odot}$ and $29_{-4}^{+4} M_{\odot}$, respectively [7]. Two years later, in 2017, the first gravitational wave signal from a binary neutron star merger event, GW170817, was detected by the LIGO and Virgo detectors [8]. The total mass of the neutron star binary is $2.74_{-0.01}^{+0.04} M_{\odot}$. A short gamma-ray burst (GRB 170817A) was observed 1.7 s after the coalescence time, which is believed to be the electromagnetic counterpart of GW170817 [9, 10]. For the gravitational wave emission from binary neutron star mergers, it is interesting that the tidal effect will change the wave form to some extent, thus it is possible to diagnose the EoS of neutron stars with the so called tidal deformability [11]. In this way, the observations of GW170817 have provided us with the first constraint on neutron star tidal

deformability, which is an extremely useful feature for studying neutron star EoS [12–19].

The tidal deformability also could be used to distinguish between strange quark stars and neutron stars. According to a longly existed hypothesis, strange quark matter may be the true ground state of baryon matter, so the observed pulsars may actually be strange quark stars [20–23]. Due to the special nature of quark stars, they have very different mass - radius relations [24]. But for a $1.4 M_{\odot}$ strange star, its radius is very similar to that of a typical $1.4 M_{\odot}$ neutron star, which makes it very difficult to distinguish quark stars from neutron stars observationally. It is interesting to note that quark stars rely on strong interactions to restrain themselves rather than solely on gravity. It means that there could be strange quark planets in the universe [20, 21, 25]. Furthermore, it even allows a strange dwarf to exist, in the form of a strange quark core covered by a normal matter crust [26, 27]. At the center of a strange quark dwarf, the density will be 100 — 1000 times larger than that of normal white dwarfs. Interestingly, some possible phenomena associated with the crust collapse of strange quark stars have been studied [28–31].

The tidal deformability of strange quark stars has been calculated by several groups [32–34]. For strange stars and neutron stars, this parameter again is quite similar at $1.4 M_{\odot}$. It shows some difference mainly at the low mass end. We thus need to pay attention to some more special merger events. It has been argued that the gravitational wave signal from the merger of a strange planet with a strange star in the Milky Way could be detected by the LIGO detector, and it could even be detected by the next-generation Einstein Telescope when the merger happens in local galaxies up to several Mpc [35, 36]. Strange planets and strange dwarfs are hopeful candidates that could be used to test the strange quark matter hypothesis [37–39], but their tidal deformability has not been thoroughly in-

* hyf@nju.edu.cn

vestigated. Here we will calculate the tidal deformability of strange quark planets and strange dwarfs. Our study is aimed at merger events of strange star - strange planet systems and strange star - strange dwarf systems.

This paper is structured as follows. In Section II, we introduce the tidal deformability and the method to calculate them. In Section III, we present our numerical results for strange dwarfs and strange planets. The combined tidal deformability of strange quark binaries is also calculated. Finally, Section IV is our conclusion and discussion.

II. METHOD

A. Tidal deformability

In a strong tidal field, the structure of a compact object will be distorted. Tidal deformability is used to measure this distortion, which is defined as the ratio of one star's induced quadrupole moment Q_{ij} with respect to its companion's tidal field E_{ij} , i.e., [40, 41]

$$\lambda = -\frac{Q_{ij}}{E_{ij}}. \quad (1)$$

Sometimes we use a dimensionless tidal deformation parameter defined as,

$$\Lambda = \frac{\lambda c^{10}}{G^4 m^5}, \quad (2)$$

where m is the mass of the star, G is the gravitational constant and c is the speed of light.

The quantities that can be directly measured from gravitational wave observations are the combined tidal deformability and the chirp mass \mathcal{M} , which are related to the tidal deformability and the mass of each star in the compact binary as [8, 13],

$$\mathcal{M} = \frac{(m_1 m_2)^{3/5}}{M^{1/5}}, \quad (3)$$

$$\tilde{\lambda} = \frac{1}{26} \left[\frac{m_1 + 12m_2}{m_1} \lambda_1 + \frac{m_2 + 12m_1}{m_2} \lambda_2 \right]. \quad (4)$$

Here, m_1 and m_2 are the mass of each object, and $M = m_1 + m_2$ is the total mass of the compact star binary. We assume $m_1 > m_2$ and use $q = m_2/m_1 < 1$ to characterize their mass ratio. In Eq.(4), λ_1 and λ_2 are the tidal deformability of each object. Similarly, we can define a dimensionless combined tidal deformability as [8, 13]

$$\tilde{\Lambda} = \frac{16}{13} \frac{(m_1 + 12m_2)m_1^4 \Lambda_1 + (m_2 + 12m_1)m_2^4 \Lambda_2}{(m_1 + m_2)^5}. \quad (5)$$

A star with a large radius and a small mass will be easily distorted in the tidal field, so its tidal deformability is large. On the contrary, a compact object with a smaller radius and

a larger mass will be less distorted in the tidal field, so its tidal deformability is small [11]. The tidal deformability is uniquely determined by the EoS. Combining the EoS and the Tolman-Oppenheimer-Volkoff (TOV) equation, the tidal deformability can be numerically calculated. On the other hand, the tidal deformability can be inferred from the gravitational wave signal in the final stage of the merging process. At this stage, because the distance between the two objects is very small, the distortion due to the tidal effect from their companion is large, which will finally affect the phase evolution of the gravitational waveform. Therefore, the EoS of the object can be hinted by analyzing the gravitational wave signals. The dimensionless tidal deformability of the $1.4 M_\odot$ neutron star is constrained to be less than 800 from the observation of GW170817 [8]. The result has ruled out some stiff compact star models [42].

B. Calculation of the tidal deformability

The tidal Love number k_2 is also a key parameter that describes the change in the quadrupole of a star in the tidal field. It is related to the tidal deformability by [43, 44]

$$\lambda = \frac{2R^5}{3G} k_2 \quad (6)$$

k_2 itself can be calculated from

$$k_2 = \frac{8C^5}{5} (1-2C)^2 [2+2C(y-1)-y] [2C[6-3y+3C(5y-8)] + 4C^3[13-11y+C(3y-2)+2C^2(1+y)] + 3(1-2C)^2[2-y+2C(y-1)] \ln(1-2C)]^{-1}. \quad (7)$$

Here, R is the radius of the star and $C = Gm/Rc^2$ is its compactness parameter. The quantity $y = y(R)$ is the solution of the following differential equation from the quadrupole metric perturbation [32, 33, 44, 45],

$$ry'(r) + y(r)^2 + F(r)y(r) + Q(r) = 0, \quad (8)$$

where $F(r)$ and $Q(r)$ are give by [32, 33, 44]

$$F(r) = \frac{1 - 4\pi Gr^2(\varepsilon(r) - p(r))/c^4}{1 - 2Gm(r)/(rc^2)} \quad (9)$$

and

$$Q(r) = \frac{4\pi Gr^2/c^4}{1 - 2Gm(r)/(rc^2)} \left[5\varepsilon(r) + 9p(r) + \frac{\varepsilon(r) + p(r)}{c_s(r)^2} c^2 - \frac{6c^4}{4\pi r^2 G} \right] - 4 \left[\frac{Gm(r)/(rc^2) + 4\pi r^2 G p(r)/c^4}{1 - 2Gm(r)/(rc^2)} \right]^2. \quad (10)$$

In the above equations, $p(r)$ and $\varepsilon(r) = \rho(r)c^2$ are pressure and energy density at radius r . $c_s = c\sqrt{dp/d\varepsilon}$ is the sound

speed. These equations need to be solved together with the Tolman-Oppenheimer-Volkoff equation,

$$\frac{dp(r)}{dr} = -\frac{G\varepsilon(r)m(r)}{c^2r^2} \left[1 + \frac{p(r)}{\varepsilon(r)}\right] \left[1 + \frac{4\pi p(r)r^3}{c^2m(r)}\right] \left[1 - \frac{2Gm(r)}{c^2r}\right]^{-1}, \quad (11)$$

and

$$\frac{dm(r)}{dr} = 4\pi r^2 \rho(r). \quad (12)$$

The boundary conditions of this set of equations are $m(0) = 0$, $p(0) = p_c$, $\varepsilon(0) = \varepsilon_c$ and $y(0) = 2$ [32, 33, 46], where p_c and ε_c are the pressure and energy density at the center of the star.

Postnikov et al. pointed out that Eq.(7) will be invalid when C is very small, like in the case of strange dwarfs and strange planets [32, 33]. So, when $C < 0.1$, we use a Taylor series of Eq.(7) to calculate k_2 [32, 33], which is

$$\begin{aligned} k_2 = & \frac{(1-2C)^2}{2} \left[\frac{2-y}{3+y} + \frac{(-6+6y+y^2)C}{(3+y)^2} \right. \\ & + \frac{(12-8y+34y^2+y^3)C^2}{7(3+y)^3} \\ & + \frac{(36+48y+84y^2+62y^3+y^4)C^3}{7(3+y)^4} \\ & + \frac{5(648+1476y+1884y^2+1472y^3+490y^4+5y^5)C^4}{147(3+y)^5} \\ & \left. + o(C^5) \right]. \quad (13) \end{aligned}$$

When $C \rightarrow 0$, Eq.(8) and Eq.(7) return to the Newtonian case [47], i.e.,

$$ry'(r) + y(r)^2 + y(r) - 6 + 4\pi Gr^2 \frac{\rho}{c_s(r)^2} = 0, \quad (14)$$

and

$$k_2 = \frac{1}{2} \left(\frac{2-y}{3+y} \right). \quad (15)$$

In the case of strange quark objects covered by a nuclear matter crust, phase transition occurs and a discontinuity of density will exist inside the star. It will affect the calculation of k_2 . In this case, y around the discontinuity is [32, 33, 46]

$$y(r_d^+) - y(r_d^-) = -\frac{\Delta\rho c^2}{m_0 c^2 / 4\pi r_d^3 + p_d}, \quad (16)$$

where r_d is the position of the discontinuity, r_d^- is the position at surface of strange quark core and r_d^+ corresponds to the bottom of the crust ($r_d^+ - r_d \rightarrow +0$, $r_d - r_d^- \rightarrow +0$). In Eq.(16), m_0 is the mass of the inner strange quark core, $\Delta\rho = \rho(r_d^-) - \rho(r_d^+)$, and p_d is the pressure at r_d .

For a given equation of state, we can use the above method to solve the TOV function (Eq.(11), Eq.(12)) and the metric function (Eq.(8)) together to get the solution of $y(R)$. Then we

substitute $y(R)$ into Eq.(7) and Eq.(6) so as to get the tidal love number and the tidal deformability.

III. RESULTS

We use the phenomenological bag model to describe the strange quark matter, for which the chemical equilibrium is maintained by weak interactions. Assuming the mass of strange quarks to be zero, the EoS of the bag model is [20]

$$p = \frac{1}{3}(\varepsilon - 4B), \quad (17)$$

where B is the bag constant which represents the pressure just below the surface. According to strange quark hypothesis, the bag constant is limited by $145\text{MeV} < B^{1/4} < 162\text{MeV}$ ($57\text{MeV}/\text{fm}^3 < B < 90\text{MeV}/\text{fm}^3$)[48]. In our calculations, we assume $B = 57, 70, 80, 90\text{MeV}/\text{fm}^3$ to illustrate the effect of the bag constant on the tidal deformability of strange quark stars.

A strange quark object is consisted of a strange core and a normal matter crust. Since the density of the crust is lower than the nuclear saturation density, we use the Baym-Pethick-Sutherland (BPS) [49] equation of state to describe it. The pressure (p_d) at the boundary between the core and the crust is an important parameter. It determines the values of $\rho(r_d^-)$ and $\rho(r_d^+)$. $\rho(r_d^+)$ must be smaller than the neutron drip density of $4.3 \times 10^{11} \text{ g/cm}^3$, which surely is the ultimate maximum density that the crust could reach [26, 27, 50]. In 1997, Huang et al. pointed out that when the $\rho(r_d^+)$ reaches $\sim 8.3 \times 10^{10} \text{ g/cm}^3$, the gap between the crust and the quark core will be too small to support the crust [51]. So, in our calculations, we will take $\rho(r_d^+) = 8.3 \times 10^{10} \text{ g/cm}^3$.

A. Tidal deformability of bare strange quark objects

The tidal deformability of strange stars whose masses exceed $0.1 M_\odot$ has been extensively studied by several groups [32–34]. In this study, we will mainly focus on the tidal deformability of less massive strange quark stars, i.e. strange quark planets and dwarfs. Here, we first concentrate on bare strange objects. Using the EoS described above, we have calculated the structure and the tidal deformability of bare strange quark stars. In Fig. 1, we show the tidal deformability and the dimensionless tidal deformability as a function of mass. From the upper panel, we see that as the mass increases, the tidal deformability also increases in most of the mass range. The tidal deformability of a strange star of $1.4 M_\odot$ is about 1000 times larger than that of a strange quark planet of about one Jupiter mass. It means that in the tidal field, bare strange quark planets deform much less than massive bare strange quark stars. Additionally, when a larger bag constant is assumed, the tidal deformability becomes smaller. This is also easy to understand, since a larger bag constant generally leads to a larger mean density, which will make the

object less deformed in the tidal force field. The lower panel of Fig. 1 illustrates the dimensionless tidal deformability versus the stellar mass. It is interesting to note that the dimensionless tidal deformability continue to decrease as the mass increases in most of the mass range. This tendency is very different from that shown in the upper panel.

Inside bare strange quark planets and dwarfs, the density does not vary too much so that it can be regarded as a constant ($\bar{\rho}$). Then the relationship between the total mass and radius is

$$m = \frac{4}{3}\pi R^3 \bar{\rho}. \quad (18)$$

At the same time, the numerical calculation indicates that k_2 is also always close to 0.75. Then, the tidal deformability can be analytically derived as,

$$\lambda = \frac{1}{2G} \left(\frac{3}{4\pi\bar{\rho}} \right)^{\frac{5}{3}} m^{\frac{5}{3}}, \quad (19)$$

and

$$\Lambda = \frac{c^{10}}{2G^5} \left(\frac{3}{4\pi\bar{\rho}} \right)^{\frac{5}{3}} m^{-\frac{10}{3}}. \quad (20)$$

It means that the theoretical slopes of the curves in the upper and lower panels should be $5/3$ and $-10/3$, correspondingly. Our numerical results are consistent with these theoretical expectations.

B. Tidal deformability of strange quark objects with crust

Fig. 2 plots the mass-radius relation and mass-central density (ρ_c) of strange quark stars with crust. The whole sequence includes strange stars, strange dwarfs and strange planets, compared with normal white dwarfs and normal planets. Note that those objects in the dotted segment are unstable[52]. All other segments of the strange dwarf/strange planet curve are stable against radial oscillations because of the existence of the quark core [26, 27]. In the mass-central density panel, the left branch corresponds to normal planets and normal white dwarfs, while the right branch corresponds to strange quark objects of different masses. We see that the central density of strange objects is always larger than $4.1 \times 10^{14} \text{ g/cm}^3$. This is easy to understand. For these objects, whenever there is a strange quark matter core, the central density will definitely be higher than $4B$ (see the EoS of Eq. (17)), which is just the above density value.

We have also calculated the tidal deformability of the whole strange quark object sequence. The results are shown in Fig. 3. Comparing with a $1.0 - 2.0 M_\odot$ strange star, a strange dwarf/planet has a smaller mass and a much larger radius. Consequently, it has a much smaller mean density and will be easily deformed in a tidal field, which means a strange dwarf/planet will have a much larger tidal deformability as compared with a $1.0 - 2.0 M_\odot$ strange star. This can be clearly seen in both panels of Fig. 3. For a strange dwarf,

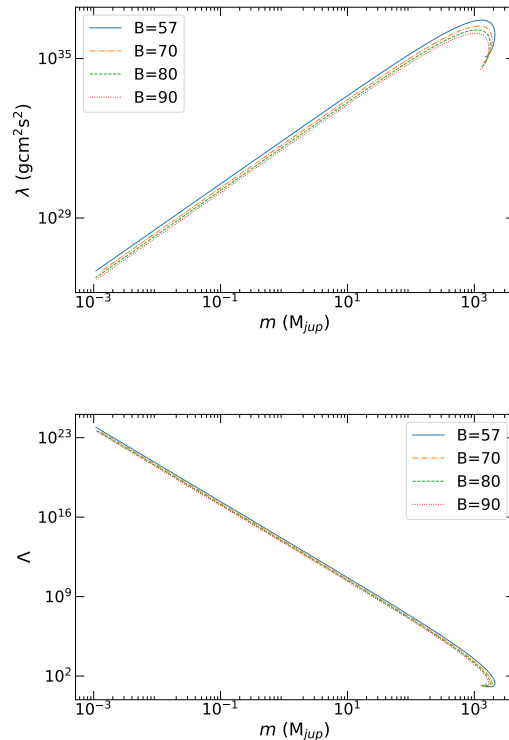


FIG. 1. Tidal deformability (the upper panel) and dimensionless tidal deformability (the lower panel) versus the stellar mass for bare strange quark stars. Different line styles represent different bag constant, which are marked in the figure in units of MeV/fm^3 . The stellar mass is in units of Jupiter mass (M_{jup}).

when the mass is larger than $\sim 0.1 M_\odot$, the crust is generally not too thick and it does not significantly affect the tidal deformability. As a result, the tidal deformability does not differ too much for a strange dwarf and a normal white dwarf when their masses are larger than $0.1 M_\odot$. This is consistent with previous researches by Postnikov et al. [32]. Anyway, we note that the tidal deformability of strange dwarfs is still generally less than that of white dwarfs of the same mass. For example, at the typical mass of $\sim 0.6 M_\odot$, the tidal deformability of a strange dwarf is about 1.4 times less than that of a normal white dwarf. In short, a strange quark object generally has a smaller tidal deformability as compared with its normal matter counterpart. Gravitational wave observations thus can effectively help us identify strange quark objects, especially strange dwarfs/planets [35, 36].

C. Binary parameters

The tidal deformability affects the phase evolution of gravitational wave signal. This effect can be measured by the combined tidal deformability $\tilde{\lambda}$ [44]. On one hand, the combined tidal deformability can be directly obtained from gravitational wave observations [44]. On the other hand, from Eq.(5), we

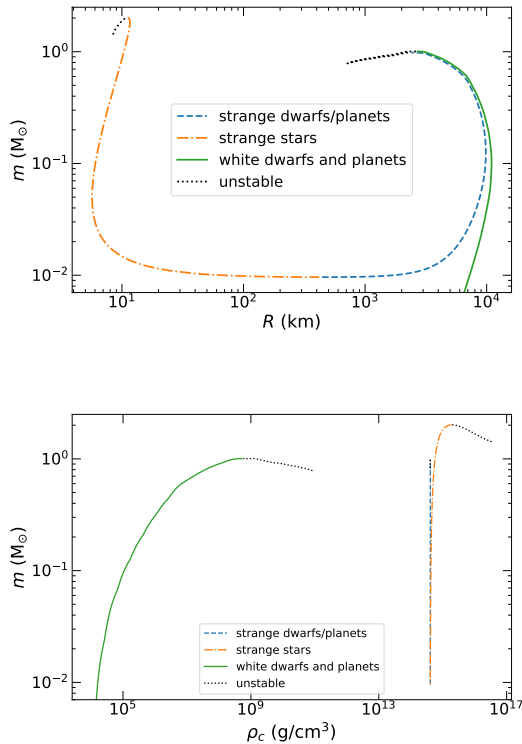


FIG. 2. Stellar mass versus radius (the upper panel) and stellar mass versus mass-central density (the lower panel) for the whole sequence of strange quark objects with crust. The dash-dotted segment represents strange quark stars (which are the counterparts of classical neutron stars). The dashed segment represents strange dwarfs and strange planets. The solid segment represents normal white dwarfs and normal planets. The dotted segment represents unstable branch. The bag constant is taken as $B=57 \text{ MeV/fm}^3$.

see that the combined tidal deformability can be calculated by considering the tidal deformability and mass of each object in the compact star binary [8, 13].

In our study, we have calculated the combined tidal deformability of strange star binaries. For the mass of the primary compact star in the binary system, we have taken three typical values, i.e., $1.0 M_\odot$, $1.4 M_\odot$ and $2.0 M_\odot$. The companion is assumed to have a smaller mass, characterized by the mass ratio q . When the companion's mass is very low, it is a strange planet and the binary become a strange star - strange planet system. We consider the two cases that the strange quark objects are either bare strange stars or covered with a crust.

For bare strange quark stars, our numerical results on $\tilde{\lambda}$ and $\tilde{\Lambda}$ are shown in Fig. 4. We see that when the companion becomes less massive, the combined tidal deformability generally decreases continuously. For the strange star-strange planet systems, the combined tidal deformability is about $\sim 10^{35} \text{ g cm}^2 \text{ s}^2$, which is much smaller than that of binary neutron star systems (which is $\sim 10^{36} \text{ g cm}^2 \text{ s}^2$). Note that the curves become flat at the low mass-ratio regime, which means the combined tidal deformability is largely indepen-

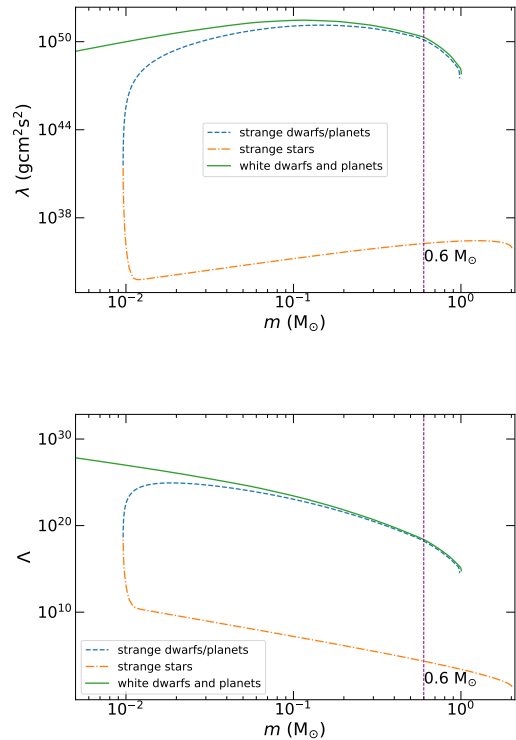


FIG. 3. Tidal deformability (the upper panel) and dimensionless tidal deformability (the lower panel) of strange quark objects with crust. Line styles and parameters are the same as those in Fig. 2. For clarity, the unstable branch is not shown in this plot.

dent of the planet mass.

Fig. 5 illustrates our results on $\tilde{\lambda}$ and $\tilde{\Lambda}$ for strange quark stars with crust. In this figure, both the primary star (assumed to be of $1.4 M_\odot$) and the smaller companion are covered by a crust. Since we are mainly interested in the gravitational wave features of strange star-strange planet systems, we also plot the combined tidal deformability of compact star-normal white dwarf/normal planet systems for comparison. From this figure, we can draw at least two conclusions. First, we see that the combined tidal deformability of the strange star-strange planet/strange dwarf systems now is generally in the range of $10^{49} \text{ g cm}^2 \text{ s}^2 - 10^{51} \text{ g cm}^2 \text{ s}^2$, it is much larger than that of binary neutron star systems (which is $\sim 10^{36} \text{ g cm}^2 \text{ s}^2$). This is very different from the case of bare strange quark objects, but it is easy to understand. When the strange planet/dwarf has a crust, its radius will be significantly increased so that it will be much sensitive to the tidal effect. Second, when the companion mass is larger than $\sim 0.1 M_\odot$, the difference between a strange star-strange dwarf system and a neutron star-white dwarf system is not significant. However, when the companion mass is less than $\sim 0.1 M_\odot$, the difference between the solid curve and the dashed curve becomes very significant.

In order to show the effect of tidal deformation on the gravitational waveform signal, we calculate the accumulated phase

of different systems by [44]

$$\frac{d\Phi}{dx} = -\frac{195c^{15/3} x^{3/2} \tilde{\lambda}}{8G^{7/3} M^5 \eta}, \quad (21)$$

where $x = (\omega M)^{2/3}$ is a dimensionless post-Newtonian parameter, ω is the orbital angular frequency and $\eta = m_1 m_2 / M^2$ is the symmetric mass ratio. The accumulated phases of some representative systems are considered, including a binary strange star system ($m_1 = m_2 = 1.4 M_\odot$, $\tilde{\lambda} = 2.7 \times 10^{36} \text{ g cm}^2 \text{ s}^2$), a strange star-strange planet system ($m_1 = 1.4 M_\odot$, $m_2 = 1.0 M_{\text{jup}}$, $\tilde{\lambda} = 1.7 \times 10^{35} \text{ g cm}^2 \text{ s}^2$), and a strange star-strange dwarf system ($m_1 = 1.4 M_\odot$, $m_2 = 0.6 M_\odot$, $\tilde{\lambda} = 1.5 \times 10^{50} \text{ g cm}^2 \text{ s}^2$). Three different binary neutron star systems ($m_1 = m_2 = 1.4 M_\odot$, $\tilde{\lambda}_1 = 1 \times 10^{36} \text{ g cm}^2 \text{ s}^2$, $\tilde{\lambda}_2 = 5 \times 10^{36} \text{ g cm}^2 \text{ s}^2$, $\tilde{\lambda}_3 = 10 \times 10^{36} \text{ g cm}^2 \text{ s}^2$), note that the different $\tilde{\lambda}_i$ here corresponds to different EoS of neutron stars) and a neutron star-white dwarf system ($m_1 = 1.4 M_\odot$, $m_2 = 0.6 M_\odot$, $\tilde{\lambda} = 2.0 \times 10^{50} \text{ g cm}^2 \text{ s}^2$) are also calculated for comparison. Our numerical results are shown in Fig. 6.

From Fig. 6, we see that different EoS generally leads to different accumulated phase. However, the phase difference between binary neutron stars and binary strange stars ($1 - 2 M_\odot$) is basically very small. It would be difficult to discriminate between them by means of gravitational waveform observations. For strange planetary systems, the accumulated phase is significantly different. Note that an ordinary planet orbiting around a compact star is not an effective gravitational wave emitter, because it would be tidally disrupted by the compact host when it gets close enough. Fig. 6 further proves the idea that gravitational wave is an effective probe of strange quark planets [35, 36]. From the lower panel, we see that the accumulated phase of a neutron star-white dwarf binary is about 1.34 times of that of a strange star-strange dwarf system. Such a phase difference may hopefully be measured by the next generation gravitational wave detectors.

IV. CONCLUSION

In this study, we calculate the tidal deformability of strange quark stars, which could be either bare ones or covered by a normal matter crust. Especially, we concentrate on less massive objects, i.e., strange dwarfs and strange planets. For bare strange quark planets, since the internal density is almost constant, it is found that the tidal deformability simply scales as $\lambda \propto m^{5/3}$, while the dimensionless tidal deformability scales as $\Lambda \propto m^{-10/3}$. As for the combined tidal deformability, it is shown that this binary parameter is generally very small

for strange planetary systems, of the order of $10^{34} \text{ g cm}^2 \text{ s}^2$, which is much smaller than that of binary neutron star systems (which is $\sim 10^{36} \text{ g cm}^2 \text{ s}^2$). When the strange quark objects have a crust, it is found that the tidal deformability of strange dwarfs and strange planets are still less than that of their normal matter counterparts. The difference is especially significant for planetary objects. It means that strange quark planets will be less deformed in a tidal field as compared with a normal planet.

Our study clearly shows that it is a hopeful method to try to identify strange quark object by searching for strange quark planets through gravitational wave observations. Tidal deformability will be a useful tool to probe the internal structure of compact stars. In fact, it has been argued that the gravitational wave signals of merging strange star planetary systems in our Galaxy can be detected by advanced-LIGO. Encouragingly, in the future, such signals from local galaxies up to several Mpc will even be detectable to the Einstein Telescope [35, 36].

It is an interesting problem that how strange quark planets/dwarfs can be formed in the Universe. Theoretically, there are at least two possibilities. First, they may be born together with their host, i.e. the primary strange quark star. The primary strange quark star itself may be produced due to an accretion-induced phase transition of a neutron star, or during a binary neutron star merger. During these fierce processes, a lot of small chunks of quark matter, which is called ‘‘strangelets’’, will be ejected. They will contaminate surrounding ordinary planets/white dwarfs and produce strange quark planets/dwarfs. Furthermore, since the newly formed strange quark star is fast spinning and highly turbulent, it may also eject some large clumps (of planetary mass) to directly produce strange quark planets around it [53, 54]. Second, there is a stage in the early Universe called the quark-gluon phase. At this stage, denser clumps of planetary mass or dwarf mass may form directly. They may survive to the present and be captured by other stars to form planetary systems or strange dwarf binaries [55].

ACKNOWLEDGEMENTS

We thank the anonymous referee for helpful comments and suggestions that lead to an overall improvement of this study. This work is supported by National SKA Program of China No. 2020SKA0120300, by the National Natural Science Foundation of China (Grant Nos. 11873030, 12041306, U1938201, 12103055, 11903019, 11833003), and by the science research grants from the China Manned Space Project with NO. CMS-CSST-2021-B11.

[1] P. Danielewicz and J. Lee, Nuclear Physics A, 922, 1 (2014).
[2] A. W. Steiner, J. M. Lattimer, and E. F. Brown, The Astrophysical Journal, 722, 33 (2010).

[3] G. Baym and C. Pethick, Annual Review of Astronomy and Astrophysics, 17, 415 (1979).
[4] J. M. Lattimer and M. Prakash, Science, 304, 536 (2004).
[5] B. P. Abbott, et al., Physical Review X, 6, 041015 (2016).

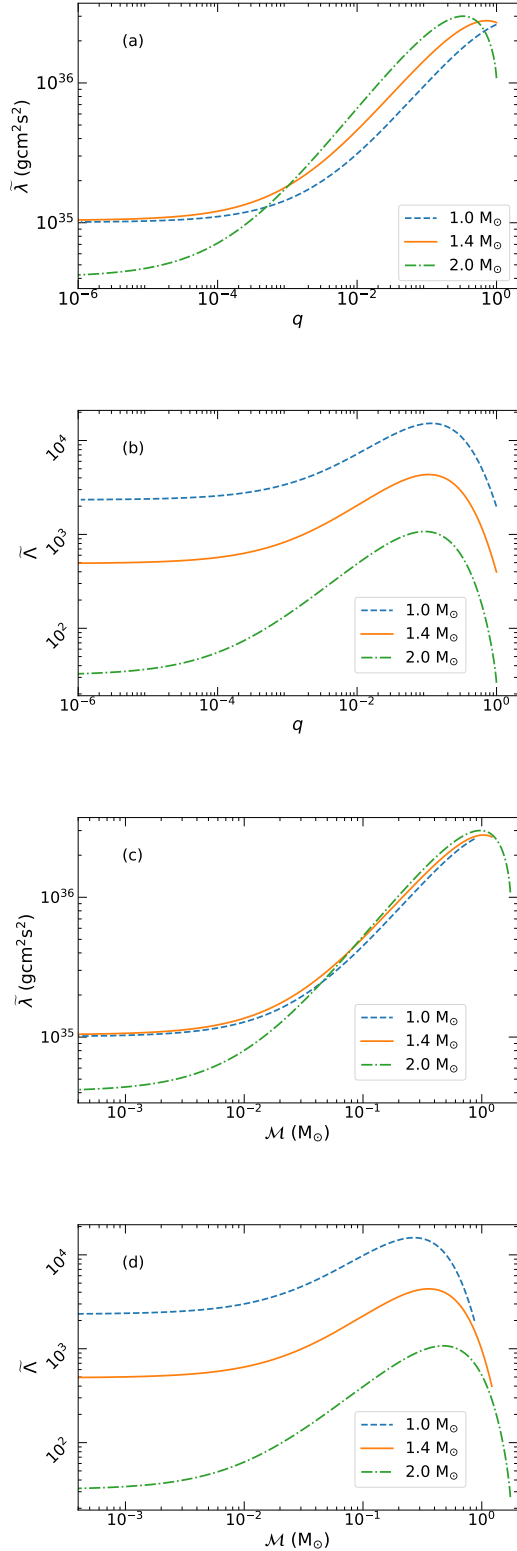


FIG. 4. The combined tidal deformability (a) and combined dimensionless tidal deformability (b) as a function of the mass ratio q for bare strange quark objects. In Panels (c) and (d), the combined tidal deformability and combined dimensionless tidal deformability are plot versus the chirp mass \mathcal{M} . The mass of the primary strange quark star is marked in each panel.

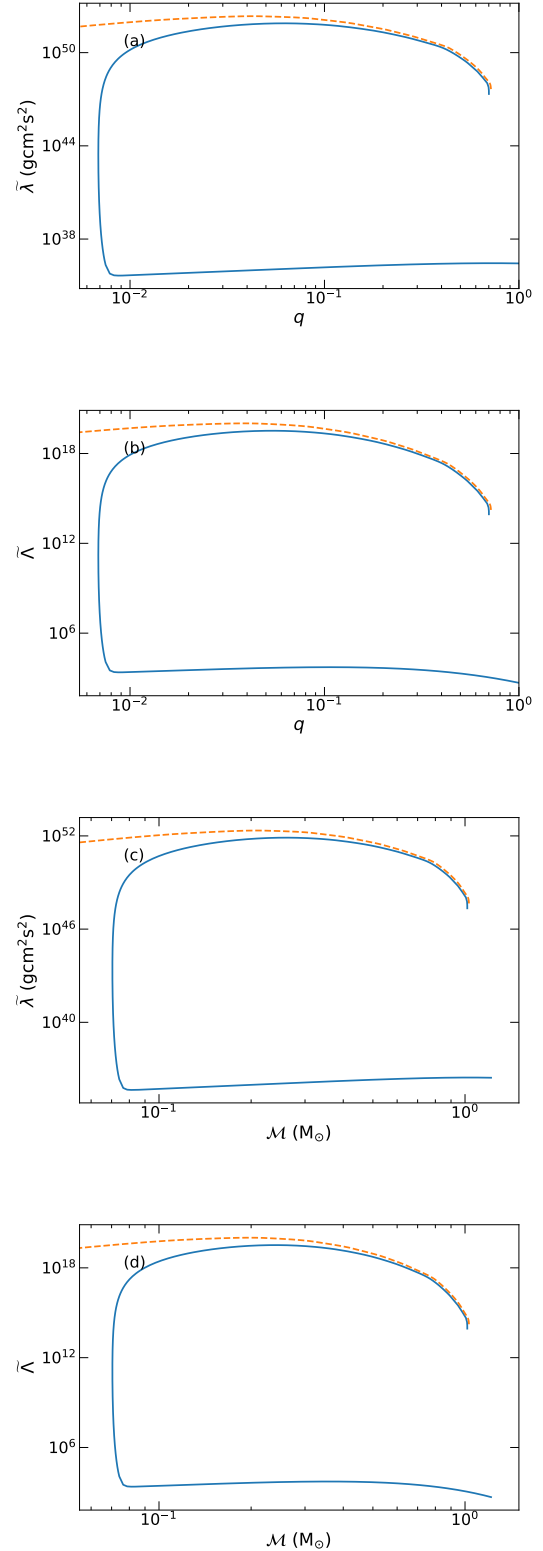


FIG. 5. The combined tidal deformability (a) and combined dimensionless tidal deformability (b) as a function of the mass ratio q for strange quark objects with crust. In Panels (c) and (d), the combined tidal deformability and combined dimensionless tidal deformability are plot versus the chirp mass \mathcal{M} . For comparison, the dashed curve illustrates the case of pulsar-white dwarf/normal planet systems. In all the plot, the primary compact star is assumed to have a mass of $1.4 M_{\odot}$. For clarity, the unstable branch is not shown in this plot.

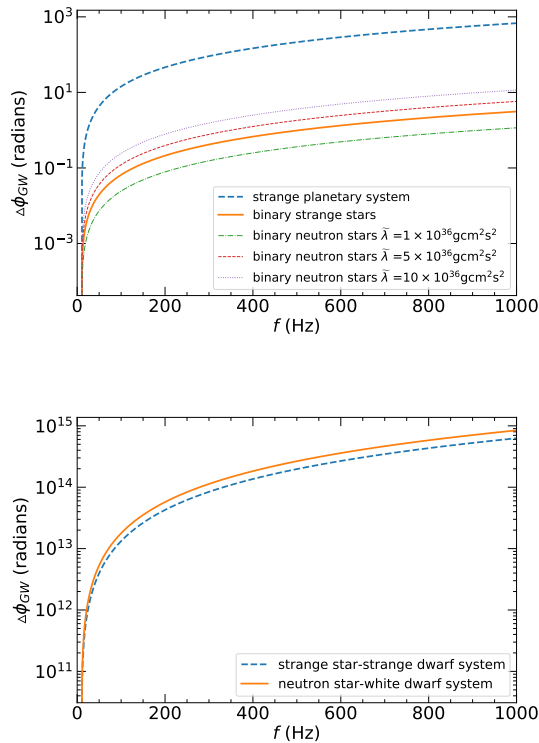


FIG. 6. The accumulated phase versus gravitational wave frequency for binary strange stars and strange planetary systems (the upper panel). The lower panel shows the case for a strange star-strange dwarf binary. For comparison, the accumulated phase of binary neutron star systems (with different combined tidal deformability, which corresponds to different EoS) and neutron star-white dwarf systems is also plot correspondingly. The calculation of the accumulated phase starts at 10 Hz in all the cases.

[6] B. P. Abbott, et al., *Physical Review Letters*, 116, 221101 (2016).
 [7] B. P. Abbott, et al., *Physical Review Letters*, 116, 241102 (2016).
 [8] B. P. Abbott, et al., *Physical Review Letters*, 119, 161101 (2017).
 [9] B. P. Abbott, et al., *The Astrophysical Journal*, 848, L12 (2017).
 [10] B. P. Abbott, et al., *The Astrophysical Journal*, 848, L13 (2017).
 [11] A. Guerra Chaves and T. Hinderer, *Journal of Physics G Nuclear Physics*, 46, 123002 (2019).
 [12] B. P. Abbott, et al., *Physical Review Letters*, 121, 161101 (2018).
 [13] B. P. Abbott, et al., *Physical Review X*, 9, 011001 (2019).
 [14] B. Margalit and B. D. Metzger, *The Astrophysical Journal*, 850, L19 (2017).
 [15] E. Annala, T. Gorda, A. Kurkela, and A. Vuorinen, *Physical Review Letters*, 120, 172703 (2018).
 [16] E. R. Most, L. R. Weih, L. Rezzolla, and J. Schaffner-Bielich, *Physical Review Letters*, 120, 261103 (2018).
 [17] S. De, D. Finstad, J. M. Lattimer, D. A. Brown, E. Berger, C. M. Biwer, *Physical Review Letters*, 121, 091102 (2018).
 [18] A. Bauswein, O. Just, H.-T. Janka, and N. Stergioulas, *The Astrophysical Journal*, 850, L34 (2017).

[19] D. Radice, A. Perego, F. Zappa, and S. Bernuzzi, *The Astrophysical Journal*, 852, L29 (2018).
 [20] E. Farhi and R. L. Jaffe, *Physical Review D*, 30, 2379 (1984).
 [21] E. Witten, *Physical Review D*, 30, 272 (1984).
 [22] A. V. Olinto, *Physics Letters B*, 192, 71 (1987).
 [23] A. Halder, S. Banerjee, S. K. Ghosh, and S. Raha, *Physical Review C*, 103, 035806 (2021).
 [24] N. K. Glendenning, *Physical Review Letters*, 63, 2629 (1989).
 [25] C. Alcock, E. Farhi, and A. Olinto, *The Astrophysical Journal*, 310, 261 (1986).
 [26] N. K. Glendenning, C. Kettner, and F. Weber, *The Astrophysical Journal*, 450, 253 (1995).
 [27] N. K. Glendenning, C. Kettner, and F. Weber, *Physical Review Letters*, 74, 3519 (1995).
 [28] K. S. Cheng, Z. G. Dai, D. M. Wei, and T. Lu, *Science*, 280, 407 (1998).
 [29] J.-J. Jia and Y.-F. Huang, *Chinese Astronomy and Astrophysics*, 28, 144 (2004).
 [30] Y. Zhang, J.-J. Geng, and Y.-F. Huang, *The Astrophysical Journal*, 858, 88 (2018).
 [31] J.-J. Geng, B. Li, and Y.-F. Huang, *The Innovation*, 2, 100152 (2021).
 [32] S. Postnikov, M. Prakash, and J. M. Lattimer, *Physical Review D*, 82, 024016 (2010).
 [33] J. Takátsy and P. Kovács, *Physical Review D*, 102, 028501 (2020).
 [34] C.-M. Li, S.-Y. Zuo, Y. Yan, Y.-P. Zhao, F. Wang, Y.-F. Huang, H.-S. Zong, *Physical Review D*, 101, 063023 (2020).
 [35] J.-J. Geng, Y.-F. Huang, and T. Lu, *The Astrophysical Journal*, 804, 21 (2015).
 [36] A. Kuerban, J.-J. Geng, and Y.-F. Huang, *Xiamen-CUSTIPEN Workshop on the Equation of State of Dense Neutron-Rich Matter in the Era of Gravitational Wave Astronomy*, AIP Conference Proceedings, 2127, 020027 (2019).
 [37] Y.-F. Huang and Y.-B. Yu, *The Astrophysical Journal*, 848, 115 (2017).
 [38] A. Kuerban, J.-J. Geng, Y.-F. Huang, H.-S. Zong, and H. Gong, *The Astrophysical Journal*, 890, 41 (2020).
 [39] A. Kuerban, Y.-F. Huang, J.-J. Geng, and H.-S. Zong, *arXiv e-prints*, arXiv:2012.05748 (2020).
 [40] É. É. Flanagan and T. Hinderer, *Physical Review D*, 77, 021502 (2008).
 [41] K. S. Thorne, *Physical Review D*, 58, 124031 (1998).
 [42] K. Chatziioannou, *General Relativity and Gravitation*, 52, 109 (2020).
 [43] A. E. H. Love, *Proceedings of the Royal Society of London Series A*, 82, 73 (1909).
 [44] T. Hinderer, B. D. Lackey, R. N. Lang, and J. S. Read, *Physical Review D*, 81, 123016 (2010).
 [45] A. Kanakis-Pegios, P. S. Koliogiannis, and C. C. Moustakidis, *Symmetry*, 13, 183 (2021).
 [46] T. Damour and A. Nagar, *Physical Review D*, 80, 084035 (2009).
 [47] T. Hinderer, *The Astrophysical Journal*, 677, 1216 (2008).
 [48] A. Schmitt, *Lecture Notes in Physics*, Berlin Springer Verlag, 811, (2010).
 [49] G. Baym, C. Pethick, and P. Sutherland, *The Astrophysical Journal*, 170, 299 (1971).
 [50] N. K. Glendenning and F. Weber, *The Astrophysical Journal*, 400, 647 (1992).
 [51] Y.-F. Huang and T. Lu, *Astronomy and Astrophysics*, 325, 189 (1997).
 [52] J. M. Bardeen, K. S. Thorne, and D. W. Meltzer, *The Astrophysical Journal*, 145, 505 (1966).

[53] R.-X. Xu and F. Wu, Chinese Physics Letters, 20, 806 (2003).

[54] J. E. Horvath, Research in Astronomy and Astrophysics, 12, 813 (2012).

[55] W. N. Cottingham, D. Kalafatis, and R. Vinh Mau, Physical Review Letters, 73, 1328 (1994).